Proteomics analysis of hip articular cartilage identifies differentially expressed proteins associated with osteonecrosis of the femoral head

Jidong Song[1#], Junlong Wu[2,1#], Blandine Poulet[3], Jialin Liang[1], Chuanyi Bai[1], Xiaoqian Dang[1], Kunzheng Wang[1], Lihong Fan[1], Ruiyu Liu[1,3*]

1 The Second Affiliated Hospital, Xi'an Jiaotong University, Xi'an, Shaanxi Province, 710004, China
2 Luoyang Central Hospital Affiliated to Zhengzhou University, Luoyang, Henan Province, 471009, China
3 Institute of Ageing and Chronic Disease, University of Liverpool, Liverpool L7 8TX, UK

Jidong Song, MD, Department of Orthopaedics, the Second Affiliated Hospital, Xi'an Jiaotong University, NO.157, Xiwu Road, Xi'an, Shaanxi, 710004, P.R.China Email address: sjidong12@stu.xjtu.edu.cn

Junlong Wu, MD, Department of Orthopaedics, Luoyang Central Hospital Affiliated to Zhengzhou University, Luoyang, Henan Province, 471009, P.R.China
Department of Orthopaedics, the Second Affiliated Hospital, Xi'an Jiaotong University, NO.157, Xiwu Road, Xi'an, Shaanxi, 710004, P.R.China Email address: xj9826375edu@163.com

Blandine Poulet, MD, Muscoskeletal Biology, Institute of Ageing and Chronic Disease, University of Liverpool, William Henry Duncan Building, West Derby Road, Liverpool, L7 8TX, UK Email address: B.Poulet@liverpool.ac.uk

Jialin Liang, MD, Department of Orthopaedics, the Second Affiliated Hospital, Xi'an Jiaotong University, NO.157, Xiwu Road, Xi'an, Shaanxi, 710004, P.R.China Email address: 1092894169@qq.com

Chuanyi Bai, MD, Department of Orthopaedics, the Second Affiliated Hospital, Xi'an Jiaotong University, NO.157, Xiwu Road, Xi'an, Shaanxi, 710004, P.R.China Email address: xjwang1934@163.com

Xiaoqian Dang, MD, Department of Orthopaedics, the Second Affiliated Hospital, Xi'an Jiaotong University, NO.157, Xiwu Road, Xi'an, Shaanxi, 710004, P.R.China Email address: dangxiaoqian@vip.163.com

Kunzheng Wang, MD, Department of Orthopaedics, the Second Affiliated Hospital, Xi'an Jiaotong University, NO.157, Xiwu Road, Xi'an, Shaanxi, 710004, P.R.China Email address: kunzheng_wang@126.com

Lihong Fan, MD, Department of Orthopaedics, the Second Affiliated Hospital, Xi'an Jiaotong University, NO.157, Xiwu Road, Xi'an, Shaanxi, 710004, P.R.China Email address: drfan2140@163.com

[#] These two authors contribute equally to this manuscript.

*Correspondence to:
Ruiyu Liu, MD, Department of Orthopaedics, the Second Affiliated Hospital, Xi'an Jiaotong University, NO.157, Xiwu Road, Xi'an, Shaanxi, 710004, P.R.China
Institute of Ageing and Chronic Disease, University of Liverpool, William Henry Duncan Building, West Derby Road, Liverpool, L7 8TX, UK
Phone number: +86 15829588608
Email address: liuryu@126.com

1. Introduction

Osteonecrosis of the femoral head (ONFH) is a refractory orthopedic disease causing progressive avascular bone necrosis and substantial loss of the hip joint function[1]. It usually affects young, active adults between the ages of 20 and 50 and progresses to collapse of the femoral head in 80% of untreated patients[2, 3]. ONFH prevalence has increased in recent decades with 20,000 to 30,000 newly diagnosed patients in the United States[2] and 8.12 million ONFH cases in China[4]. However, for the younger patients with ONFH, hip preservation treatment may be preferable as it can delay or avoid disease progression in the early-stage necrosis. Joint-preserving treatment would also benefit from inhibition of cartilage degeneration that may result from bone tissue reconstruction and the development of secondary osteoarthritis in the treated hip[5].

Most previous studies on ONFH focused on the destruction of bone tissue or bone marrow [6], the pathogenesis of articular cartilage degeneration in ONFH patients is often underappreciated. Cartilage degeneration has been found at the early stage of ONFH[7] with cartilage metabolic abnormalities seen before radiologic evidence in the femoral head necrosis[8, 9]. In addition, cartilage matrix and glycosaminoglycans (GAG) content decrease in the early-stage of the disease[10, 11]. Articular cartilage is an avascular tissue, which is nourished by materials from synovial fluid and subchondral bone[12, 13]. Subchondral bone

necrosis and further collapse could lead to interruption of nutrition supply from subchondral bone to cartilage and thereby contribute to the development of cartilage degeneration in ONFH. Therefore, the mechanism of cartilage degeneration in ONFH is theoretically different from that of primary osteoarthritis (OA)[14], which is mainly related to mechanical, genetic and environmental factors, and in which articular cartilage is the primary affected tissue along with subchondral bone sclerosis, but not necrosis[15].

Understanding the molecular pathways in cartilage degeneration in early ONFH is essential for successful joint-preserving strategy. Little is known about the molecular mechanism underlying the progressive degeneration of articular cartilage in early ONFH. Previous studies explored the role of IL-9 and IL-21 in cartilage degeneration of ONFH patients and the relationship between plasma cartilage oligomeric matrix protein[16, 17] and the progression of non-traumatic ONFH[18]. These studies focused on only one or several proteins that are involved in ONFH cartilage degeneration. The expression profile of ONFH cartilage has been determined by using microarray[19], however, mRNAs alteration does not completely match with the changes of proteins since protein expression levels are dependent on the post-transcriptional regulation, post-translational modification and differential stability of proteins.

A proteomics approach, in which entire protein in tissue or cells are identified and quantified directly, has shown to be a valuable way to elucidate the molecular basis of disease etiology and pathogenesis. To better understand the mechanism involved in cartilage degeneration in ONFH, we conducted an isobaric tandem mass tag (TMT) based quantitative proteomics analysis of ONFH and fracture control cartilage. The results of this study may give new insight into the molecular basis of the pathogenesis in ONFH cartilage, and provide novel clues for the prevention and treatment of ONFH cartilage degeneration.

2. Methods

2.1 Cartilage samples

The workflow of experiment is outlined in Figure 1. Hip cartilage samples were collected from 32 subjects undergoing total hip replacement (THA). ONFH cartilage samples were harvested from 16 patients with Ficat grade III idiopathic ONFH[20]. Fracture control cartilage samples were collected from 16 sex-matched individuals with traumatic femoral neck fracture, who underwent

THA within 24 hours of fracture. All samples were collected from anterosuperior portions of the femoral head (where the cartilage had collapsed in patients with ONFH) within 2 h of THA (Figure 1). The cartilage was used only if it had intact gross appearance and was graded less than Histologic Histochemical Grading System (HHGS) histological grade 2[21]. 5 samples were excluded in the study, in which 3 samples had damaged gross appearance and 2 samples had HHGS score greater than grade 2. All patients were diagnosed by two ONFH experts with careful clinical and radiographic examination. ONFH was diagnosed only when all experts agreed with each other. The cartilage was cut into strips from surface to subchondral bone 5 mm apart in parallel, snap-frozen in liquid nitrogen and stored at -80 ℃ until subsequent protein extraction. The sample size was based on previous study[22]. In the 16 pairs of cartilage samples, 9 pairs were used for TMT analysis, 4 pairs were used for western blot analysis and 3 pairs were fixed for immunohistochemical (IHC) analysis. The basic characteristic of the study subjects was showed in Table 1.

2.2 Protein extraction, digestion and Tandem Mass Tag labeling

Protein extraction was carried out from 9 fracture and 9 ONFH cartilage samples without removal of proteoglycans and collagens. In each group, 3 samples were mixed together as 1 biological replicate. The cartilage was ground in liquid nitrogen and the power was transferred into a 5 ml EP tube. 500 μl LSDT protein lysate (4% SDS, 100 mM Tris-HCI, 100 mM DTT, pH 8.0) was added[23]. The mixture was boiled for 5 min, homogenized by ultrasound (25 W, ultrasound 3 s, interval 7 s) in ice bath for 5 min, and centrifuged at 14 000 g for 30 min. The supernatant was filtered with 0.22 μm ultrafiltration device (Corning, NY, USA) and stored at -80 ℃[24]. Protein content was quantified by BCA protein assay reagent (Bio-Rad, CA, USA) and the quality was examined by SDS-PAGE.

For protein digestion, 300 μg of protein of each sample was used following the FASP procedure[23]. For peptide labelling, 100 μg peptide mixture was labeled using TMT 6plex™ Isobaric Mass Tagging Kit (Thermo Fisher Scientific, MA, USA). Three units from the controls were labeled with tags 126, 127C and 127N, respectively, and three units from ONFH samples were labeled with tags 128C, 129N and 130N, respectively. The labeled samples were then mixed and dried in a vacuum centrifuge at room temperature.

2.3 Peptide fractionation and LC-MS/MS analysis

For peptide fractionation, the TMT-labeled peptides were subjected to High-pH Reversed-

Phase Fractionation in 1100 Series HPLC Value System (Agilent, USA) equipped with a Gemini-NX (Phenomenex, 00F-4453-E0) column (4.6×150 mm, 3 μm, 110 Å), which was eluted at a flow rate of 1 ml/min. The detailed gradient was shown in the Supplementary materials 1. The elution process was monitored by measuring absorbance at 214 nm and fractions were collected every 1 min. The collected fractions (approximately 30) were finally combined into 10 pools. Each pool was concentrated via vacuum centrifugation and reconstituted in 10 μl of 0.1% formic acid. All samples were stored at -80 ℃.

LC-MS/MS analysis was performed using Easy-nLC nanoflow HPLC system connected to Q-Exactive (Thermo Fisher Scientific, MA, USA). 1 μg of each sample was loaded onto Thermo Scientific EASY trap column (75 μm×25 cm, 5 μm, 100 Å, C18) and separated by analytical column (75 μm×25 cm, 5 μm, 100 A, C18), which was conditioned by 95% buffer A (0.1% formic acid). The separation of peptides was performed using the following gradient: 5% to 28% solvent B (0.1% formic acid in 100% ACN) for 40 min, 28-90% solvent B for 2 min and 90% solvent B for 18 min. The column was re-equilibrated to its initial highly aqueous solvent composition before each analysis.

The mass spectrometer was operated in positive ion mode. MS spectra was acquired over a range of 350-2000 m/z. Using a data-dependent top 15 method dynamically choosing the most abundant precursor ions from the survey scan of 350-2000 m/z. Survey scans were acquired at a resolution of 60,000 at 200 m/z for MS scan and 15,000 at 100 m/z for MS/MS scan. The isolation window was 2 m/z and normalized collision energy was 35 eV. The maximum ion injection times were set at 50 ms for the survey scan and 100 ms for the MS/MS scans, and the automatic gain control target values for full scan modes was set to 1 e^6 and for MS/MS was 5 e^4. The dynamic exclusion duration was 30 s.

2.4 Database search

All raw files were searched and identified using MASCOT search engine and Proteome Discoverer 2.3 software (Thermo Fisher Scientific). The database used was uniprot_reviewed_human_20200811_20396.fasta (total 20396 sequences). The following search parameters were used: monoisotopic mass, trypsin as the digestion enzyme with allowance for a maximum of two missed cleavage, TMT labeling and carbamidomethylation of cysteine as fixed modifications, and peptide charges of 2+, 3+, and 4+, and the oxidation of

methionine were specified as variable modifications. The mass tolerance was set to 20 ppm for precursor ions and to 0.1 Da for the fragment ions. The results were filtered based on a peptide and protein false discovery rate (FDR) ≤1%. The relative quantitative analysis of the sample proteins was based on TMT reporter ion ratios from all unique peptides representing each protein. The relative peak intensities of the TMT reporter ions released in each of the MS/MS spectra were used. Only unique peptides obtained with a confidence percentage of >95% were included in. The ratio ≥1.50, or ≤0.67-fold cutoff value was used to identify upregulated or downregulated proteins with $P < 0.05$. Statistical analysis was conducted using Student T-test.

2.5 Bioinformatics analysis

Principal components analysis (PCA) was used to test the homogeneity within groups and heterogeneity between groups. It was carried out on the protein intensities using SIMCA-P+ software (v11.0, Umetrics, Umeå, Sweden). In order to characterize the function of the identified proteins, differentially expressed proteins (DEPs) in ONFH cartilage were entered to the DAVID database (http://david.abcc.ncifcrf.gov) for functional classification and Gene Ontology (GO) enrichment analysis. Pathways were elucidated according to the Kyoto Encyclopedia of Genes and Genomes (KEGG) database (http://www.kegg.jp/kegg/pathway.html). The protein-protein interaction (PPI) networks were generated through string database (http://string.embl.de) and visualized with cytoscape web application (Version 1.0.4, http://www.cytoscape.org), based on information gained up to 4 level of functional analysis: fold change of protein, PPI, KEGG pathway enrichment and biological process enrichment.

2.6 Verification by western blot

Extracted cartilage proteins were separated by 12% SDS-PAGE and transferred onto PVDF membranes (Millipore). The membranes were then blocked with 5% skim milk in TBST for 2 h at room temperature and further incubated with primary antibodies against alpha-2-HS-glycoprotein (AHSG) (16571-1-AP, Proteintech, 1:500) and cytokine-like protein 1 (Cytl1) (ab136012, Abcam, 1:00) overnight at 4 °C. After washing (5 min×4) with TBST, the membranes were incubated with 1:5000-diluted Goat anti-Mouse (or anti-Rabbit) HRP-conjugated secondary antibodies (W10808, W10809, Invitrogen, MA, USA) for 1 h at room temperature. After additional four washes, the membranes were developed by ECL kit (Bio-

Rad, Hercules, CA). Quantitative analysis of protein bands was conducted using ImageJ software (NIH, USA).

2.7 Histochemical and IHC analysis

The paraformaldehyde-fixed cartilage tissues were rinsed with PBS, decalcified with 10% EDTA, and embedded in paraffin. Five μm thick sections were dewaxed with xylene, hydrated with graded ethanol, stained respectively with hematoxylin and eosin (HE), safranin O (SO) and toluidine blue (TB) (Figure 1). For IHC staining, the hydrated sections were treated with 3% H_2O_2 for 10 min to quench the endogenous peroxidase activity, blocked with 5% BSA for 1 h, and incubated with AHSG (16571-1-AP, Proteintech, 1:300), Cytokine-like protein 1 (ab136012, Abcam, 1:100), aggrecan (bs-1223R, Bioss, 1:400) and MMP13 (bs-10581R, Bioss, 1:400) antibody at 4 ℃ overnight. After washing with PBS, the sections were incubated with secondary antibodies (SP-9001, ZSGB-BIO, China) at 37 ℃ for 30 min and stained with diaminobezidin (DAB). Negative staining controls were achieved by replacing the primary antibodies with Rabbit IgG control. For densitometric analyses, at least four sections from each cartilage specimen were quantified. The percentages of positive chondrocytes in 1000 chondrocytes were calculated and the mean percentage of positive chondrocytes was reported for each specimen. The rates of staining area of SO and TB staining and the positive staining zones of aggrecan were analyzed using ImageJ software with threshold. The superficial zone and deep zone of articular cartilage were scored separately. The Shapiro-Wilk test was used to test the Gaussian distribution and the Levene's test was used to test the homogeneous variance. The data satisfied the condition of *t*-test then the statistical analyses were performed by the *t*-test. $P < 0.05$ was considered statistically significant.

3. Results

3.1 Differentially expressed proteins identification in ONFH cartilage

PCA results showed the homogeneity and heterogeneity in and between ONFH and control groups (Figure S1). In this study, a total of 2176 proteins with 10416 unique peptides were identified in human hip cartilage. 303 DEPs were identified in ONFH cartilage when compared to fracture control. Of these proteins, 72 proteins were upregulated and 231 proteins were downregulated in this disease cartilage. The top 20 upregulated and downregulated DEPs are

listed in Table 2 and Table 3, respectively. A complete list of expressed proteins is shown in the Supplementary Table 1 (all upregulated proteins in ONFH cartilage), Supplementary Table 2 (all downregulated proteins in ONFH cartilage) and Supplementary Table 3 (all identified proteins in hip cartilage).

From these DEPs, extracellular matrix proteins related to collagen and proteoglycan include upregulation of various collagens (COL3A1, COL5A1, COL5A2, COL6A1, COL6A3 and COL15A1), and downregulation of aggrecan core protein and proteoglycan 4 in ONFH cartilage. There is no significantly difference of COL2A1 between ONFH and fracture control cartilage. A significant increase in the matrix degrading enzymes matrix metalloproteinases 2 (MMP2) and MMP13 were found in ONFH cartilage. However, a disintegrin and metalloproteinase with thrombospondin motifs-5 (ADAMTS5), which is responsible for cleaving aggrecan, and the enzymes that involved in chondroitin sulfate biosynthesis including chondroitin sulfate synthase 2 and chondroitin sulfotransferases (CHST), including CHST3, 12, and 14, which play an important role in the sulfation of chondroitin sulfate, were downregulated in ONFH cartilage.

In addition, protein levels of various growth factors were also significantly modified in ONFH cartilage, including downregulation of growth/differentiation factor (GDF)10, fibroblast growth factor 2 (FGF2), stromal cell-derived factor (SDF)-1 and macrophage migration inhibitory factor (MIF).

3.2 Gene ontology analysis

To understand the functions of DEPs identified in the ONFH group, they were classified using the GO enrichment analysis and further categorized into three groups: biological process, cellular component and molecular function. For biological process, the proteins were mainly involved in multicellular organismal process, single-multicellular organism process, response to chemical and system development (Figure 2). For cellular component, the proteins were mainly associated with extracellular region, extracellular region part, extracellular space and vesicle (Figure 2). For molecular function, the majority of enriched categories were associated with binding, protein binding, identical protein binding and receptor binding (Figure 2). The full GO analysis results are shown in Supplementary materials 2.

3.3 KEGG pathway and PPI analysis

KEGG pathway analysis indicated that most of these DEPs were associated with metabolic pathways, complement and coagulation cascades, ECM-receptor interaction and fluid shear stress and atherosclerosis (Figure 3A). Metabolic pathways account for the larger part of the DEPs, including the amino sugar and nucleotide metabolism, which has close relation with cartilage nutrient supply, and glycosaminoglycan biosynthesis and degradation, which was the important part of the cartilage matrix.

PPI network were conducted using the STRING database. As shown in Figure 3B, the DEPs were tightly networked and mainly enriched in the metabolic pathways, glycosaminoglycan biosynthesis, complement and coagulation cascades, ECM-receptor interaction. Glutathione S-transferase theta-2B (GSTT2B), 4-trimethylaminobutyraldehyde dehydrogenase (ALDH9A1), collagen alpha-3(VI) chain (COL6A3), chondroitin sulfate synthase 2(CHPF) and thrombospondin-1 (THBS1) appeared crucial in the regulation of differential expression of proteins.

3.4 Validation of DEPs

Based on the identified DEPs, the upregulated protein AHSG and the downregulated protein Cytl1 were selected for western blot and IHC analysis to verify their protein expression level in ONFH cartilage. These proteins were selected on the basis of high fold change as well as availability of commercial antibodies.

Western blot quantification showed that AHSG significantly increased in ONFH cartilage and Cytl1 was significantly decreased, as shown in Figure 4. These data confirm our mass spectrometry findings described above. IHC analysis indicated that the expression levels of AHSG at the superficial zone (SZ) and deep zone (DZ) of ONFH cartilage were significantly higher than that of fracture controls (Figure 5A). In contrast, the expression levels of cytl1 at the SZ and DZ of ONFH cartilage were significantly lower than that of fracture controls (Figure 5B). The IHC analysis was consistent with the WB results and validated the results obtained from the mass spectrometry analysis.

In the ONFH cartilage, the upregulation of MMP13 and downregulation of aggrecan were confirmed by IHC analysis (Figure S2), the downregulation of glycosaminoglycan (GAG) were confirmed by safranin O and toluidine blue staining (Figure S3).

4. Discussion

Based on the TMT high throughput proteomics strategy, a total of 2176 proteins were identified in hip articular cartilage. Using the 1.5-fold cutoff, we found 303 proteins were significantly differentially expressed in ONFH cartilage, of which 72 proteins were upregulated and 231 were downregulated. These DEPs may provide novel clues for understanding the pathogenesis of ONFH.

Collagens and aggrecan are the main extracellular matrix of articular cartilage. Many of these collagens were found to be upregulated in ONFH cartilage in this study, which is consistent with the gene expression profiles of ONFH cartilage[19]. The type V collagen, is closely linked to fibrosis[25], was found to be significantly upregulated in ONFH cartilage in our study, suggesting cartilage fibrosis may be present in ONFH cartilage. MMP13, which is the main enzyme able to degrade type 2 collagen, was upregulated in ONFH cartilage, however, the COL2A1 was not significantly different between the control and ONFH cartilage. A possible reason would be that ONFH chondrocytes increased synthesis the type 2 collagen, as is also found in OA chondrocytes[26]. This phenomenon and its mechanism need to be explored in the future. Aggrecan was found to be decreased in ONFH cartilage. Matrix metalloproteinases such as MMP2, MMP3 and MMP13 are elevated and have been involved in cartilage matrix degradation associated with OA[27]. In the ONFH cartilage, our study found MMP3 was not differentially expressed, but the upregulation of MMP2 and MMP13. MMP13 have been found in Ficat stage 3 ONFH cartilage[28]. MMP2 could degrade the aggrecan, and MMP13 degrades aggrecan in addition to collagen[29, 30]. Therefore, the decreased aggrecan may be related to the upregulation of MMP2 and MMP13 in ONFH cartilage. TIMPs can inhibit the catalytic ability of MMPs in the progression of OA. TIMP2 at higher levels could binds to MMP2 in a ratio of 1:1, blocking its enzyme activity[31] and was upregulated in the ONFH cartilage, possibly to block the matrix degradation activity of MMP2. It may be a protective factor to resist cartilage destruction in ONFH.

In addition to major cartilage matrix proteins and their main degradative enzymes, several secreted non-structural proteins that regulates chondrocyte function have been found. AHSG is an acute phase protein which regulates injury- and infection-elicited inflammatory responses,

conferring protection against injury and inflammatory diseases[32]. In OA patients, serum AHSG levels were negatively correlated with clinical severity and less serum AHSG correlated with more severe clinical OA[33]. The higher levels of AHSG in ONFH patients may represent an attempt to protect the cartilage from harmful inflammation factor found in early stage of ONFH. Cytl1 plays an important role in maintaining cartilage homeostasis. Cytl1-/- mice showed augmented osteoarthritic cartilage destruction compared with wild-type littermates[34] and it was downregulated during the progression of OA in animal model[34, 35]. The expression of Cytl1 were downregulated in ONFH cartilage and this may contribute to cartilage degradation.

KEGG pathway and PPI analysis indicated that most enriched canonical pathways of DEPs encompassed metabolic pathway, glycosaminoglycan biosynthesis, complement and coagulation cascades. These results may provide potential clue for further investigation of pathological mechanism of ONFH cartilage degeneration.

Cartilage nutrient supply influences the cartilage metabolism. For ONFH cartilage, the nutrient from the subchondral bone was interrupted because of the subchondral bone necrosis. Articular synovial fluid, another nutrient resource, demonstrated decreased concentrations of glucose and elevated concentrations of lactate relative to contralateral control hips in the ONFH animal model[36]. The main nutrient resource of cartilage, amino sugar and nucleotide sugar, whose metabolism is vital in cartilage matrix synthesis, was downregulated in ONFH cartilage. Intriguingly enough, levels of random glucose and hemoglobin were significantly downregulated in the serum of ONFH patients[37]. The metabolic change may be the adaption of ONFH chondrocytes under adverse conditions seen in the early ONFH. The findings of metabolic alterations in ONFH cartilage provide new insights into the pathophysiology of ONFH and reveal potential new therapeutic targets.

As the main component of cartilage matrix, GAG binds to aggrecan in cartilage matrix and plays an important role in cartilage morphogenesis and homeostasis. Our study found the decreased GAG in ONFH cartilage, which was consistent with the previous study[11]. Chondroitin sulfate (CS) is one of the two GAGs. The reduction in its content and an alteration in its sulfation is associated with cartilage degeneration in OA. CS sulfotransferases (CHST) are involved in chondroitin sulfate sulfation and link to the development of endemic OA,

Kashin-Beck disease (KBD)[38, 39]. CHST3, 12 and 14 were found to be downregulated in ONFH cartilage in this study, not the same as in OA and KBD cartilage[40]. In addition, downregulation of CHST2 was found in ONFH bones[41]. These findings support CHST as a potential therapeutic target of ONFH.

Complement and coagulation cascades was identified to be upregulated in ONFH cartilage, which reveals that they are involved in ONFH cartilage degeneration. This change was also observed in transcription analysis of bone tissue and serum proteome in patients with ONFH, respective[42, 43]. Further investigation is expected about how these pathways are involved in the development of ONFH. Cytokines are key regulators of cartilage metabolism and their levels were modified in ONFH cartilage. GDF10 is a target gene of SOX-9, which is involved in hypoxia promoting the differentiated human articular chondrocytes phenotype[44]. FGF suppresses collagen X and MMP13 expressions in OA cartilage but promotes the expression of collagen II[45]. SDF-1 induces the expression of type II collagen and GAG in bone marrow stem cells (BMSCs), which may promote the differentiation of BMSCs into chondrocytes under the cartilage microenvironment *in vivo*[46]. Human OA chondrocytes secreted 3-fold higher levels of MIF than normal chondrocytes and previous study showed reduced OA severity in aged mice with deletion of MIF[47]. Those cartilage protective cytokines, GDF10, FGF and SDF-1 were downregulated in ONFH cartilage as well as the harmful cytokine, MIF. The molecular functions of these differentially expressed cytokines and their interaction with the pathological mechanism of ONFH would warrant further studies.

There are some limitations in this study. First, The subjects in the two groups do not match each other exactly in terms of ages. ONFH patients usually age between 35 and 55 years old, while patients with femoral neck fracture are mostly over 60 years old. Obtaining cartilage samples needs qualified patients, THA performed and informed content. The fracture characteristics and sampling difficulties did not allow to collect normal hip cartilage specimens from adults with ages less than 60 years old. Therefore, it is difficult to achieve the exact age matching between the two groups. Second, the control samples were collected from patients with femoral neck fracture. The potential impact of fracture on protein expression may affect the accuracy of this study. To lessen this possible impact, all control samples were collected from patients within the 24 h of traumatic fracture. Third, further biological studies, such as

cell and animal experiments, are needed to explore the potential biological mechanism of identified proteins in the development of ONFH.

In conclusion, this study compared the protein expression profiles of hip articular cartilage in ONFH and fracture controls in a comprehensive and large-scale manner. We identified a number of DEPs and pathways between ONFH and fracture controls that may provide novel clues for pathogenesis studies of cartilage degradation in ONFH.

Acknowledgments and affiliations

Acknowledgements

Not applicable.

Authors' contributions

JDS drafted the work. RYL and JDS designed the experiments. JLL and JDS collected the samples. JLW and LHF analyzed the data. XQD, CYB and KZW interpreted the results. BP and RYL revised the work. All authors read and approved the final manuscript.

Ethical approval and consent to participate

The Human Ethics Committees approved this study (No. 2017-196). Informed consent was obtained from all individual participants included in the study.

Availability of Data and Materials

All data generated or analyzed during this study are included in this published article and its supplementary information files.

Role of funding source

This study was supported by the National Natural Scientific Foundation of China (81772411), and Key Research and Development Program of Shaanxi Province (2018SF-052, 2018SF-186).

Conflict of interest

The authors declare that they have no conflicts of interests.

References

1. Mont MA, Cherian JJ, Sierra RJ, Jones LC, Lieberman JR. Nontraumatic Osteonecrosis of the Femoral Head: Where Do We Stand Today? A Ten-Year Update. J Bone Joint Surg Am 2015; 97: 1604-1627.

2. Petrigliano FA, Lieberman JR. Osteonecrosis of the hip: novel approaches to evaluation and treatment. Clin Orthop Relat Res 2007; 465: 53-62.
3. Villa JC, Husain S, van der List JP, Gianakos A, Lane JM. Treatment of Pre-Collapse Stages of Osteonecrosis of the Femoral Head: a Systematic Review of Randomized Control Trials. Hss j 2016; 12: 261-271.
4. Zhao DW, Yu M, Hu K, Wang W, Yang L, Wang BJ, et al. Prevalence of Nontraumatic Osteonecrosis of the Femoral Head and its Associated Risk Factors in the Chinese Population: Results from a Nationally Representative Survey. Chin Med J (Engl) 2015; 128: 2843-2850.
5. Zhang QY, Li ZR, Gao FQ, Sun W. Pericollapse Stage of Osteonecrosis of the Femoral Head: A Last Chance for Joint Preservation. Chin Med J (Engl) 2018; 131: 2589-2598.
6. Jones LC, Hungerford DS. Osteonecrosis: etiology, diagnosis, and treatment. Curr Opin Rheumatol 2004; 16: 443-449.
7. Han X, Hong G, Chen L, Zhao M, Guo Y, Xu L, et al. T1 rho and T2 mapping for the determination of articular cartilage denaturalization with osteonecrosis of the femoral head: A prospective controlled trial. J Magn Reson Imaging 2019; 49: 760-767.
8. Li JK, Cheng L, Zhao YP, Guo YJ, Liu Y, Zhang W, et al. ADAMTS-7 exhibits elevated expression in cartilage of osteonecrosis of femoral head and has a positive correlation with TNF- alpha and NF- kappa B P65. Mediators Inflamm 2015; 2015: 196702.
9. Jingushi S, Lohmander LS, Shinmei M, Hoerrner LA, Lark MW, Sugioka Y, et al. Markers of joint tissue turnover in joint fluids from hips with osteonecrosis of the femoral head. Journal of Orthopaedic Research 2000; 18: 728-733.
10. Xu R, Wei B, Li J, Huang C, Lin R, Tang C, et al. Investigations of Cartilage Matrix Degeneration in Patients with Early-Stage Femoral Head Necrosis. Med Sci Monit 2017; 23: 5783-5792.
11. Zhang Q, Guo W, Chen Y, Zhao Q, Liu Z, Wang W. The Glycosaminoglycan Content of Hip Cartilage in Osteonecrosis of Femoral Head: Evaluation with Delayed Gadolinium-Enhanced Magnetic Resonance Imaging of Cartilage. Cartilage 2018: 1947603518803732.
12. Arkill KP, Winlove CP. Solute transport in the deep and calcified zones of articular cartilage. Osteoarthritis Cartilage 2008; 16: 708-714.
13. Pan J, Zhou X, Li W, Novotny JE, Doty SB, Wang L. In situ measurement of transport between subchondral bone and articular cartilage. J Orthop Res 2009; 27: 1347-1352.
14. Seo EM, Shrestha SK, Duong CT, Sharma AR, Kim TW, Vijayachandra A, et al. Tribological changes in the articular cartilage of a human femoral head with avascular necrosis. Biointerphases 2015; 10: 021004.
15. Li G, Yin J, Gao J, Cheng TS, Pavlos NJ, Zhang C, et al. Subchondral bone in osteoarthritis: insight into risk factors and microstructural changes. Arthritis Res Ther 2013; 15: 223.
16. Chen B, Liu Y, Cheng L. IL-21 Enhances the Degradation of Cartilage Through the JAK-STAT Signaling Pathway During Osteonecrosis of Femoral Head Cartilage. Inflammation 2017; 41: 595-605.
17. Geng W, Zhang W, Ma J. IL-9 exhibits elevated expression in osteonecrosis of femoral head patients and promotes cartilage degradation through activation of JAK-STAT signaling in vitro. Int Immunopharmacol 2018; 60: 228-234.
18. Gong SD, Chen XJ, Chen ZQ, He XM, Pang FX, Huang JY, et al. Elevated plasma cartilage

oligomeric matrix protein (COMP) level are associated with the progression of non-traumatic osteonecrosis of femoral head. Clin Chim Acta 2019; 490: 214-221.
19. Liu R, Liu Q, Wang K, Dang X, Zhang F. Comparative analysis of gene expression profiles in normal hip human cartilage and cartilage from patients with necrosis of the femoral head. Arthritis Res Ther 2016; 18: 98.
20. Ficat RP. Idiopathic bone necrosis of the femoral head. Early diagnosis and treatment. J Bone Joint Surg Br 1985; 67: 3-9.
21. Mankin HJ, Dorfman H, Lippiello L, Zarins A. Biochemical and metabolic abnormalities in articular cartilage from osteo-arthritic human hips. II. Correlation of morphology with biochemical and metabolic data. J Bone Joint Surg Am 1971; 53: 523-537.
22. Lourido L, Calamia V, Mateos J, Fernandez-Puente P, Fernandez-Tajes J, Blanco FJ, et al. Quantitative proteomic profiling of human articular cartilage degradation in osteoarthritis. J Proteome Res 2014; 13: 6096-6106.
23. Wiśniewski JR, Zougman A, Nagaraj N, Mann M. Universal sample preparation method for proteome analysis. Nature methods 2009; 6: 359-362.
24. Lei J, Amhare AF, Wang L, Lv Y, Deng H, Gao H, et al. Proteomic analysis of knee cartilage reveals potential signaling pathways in pathological mechanism of Kashin-Beck disease compared with osteoarthritis. Sci Rep 2020; 10: 6824.
25. Mak KM, Png CY, Lee DJ. Type V Collagen in Health, Disease, and Fibrosis. Anat Rec (Hoboken) 2016; 299: 613-629.
26. Imagawa K, de Andrés MC, Hashimoto K, Itoi E, Otero M, Roach HI, et al. Association of reduced type IX collagen gene expression in human osteoarthritic chondrocytes with epigenetic silencing by DNA hypermethylation. Arthritis Rheumatol 2014; 66: 3040-3051.
27. Akhtar N, Khan NM, Ashruf OS, Haqqi TM. Inhibition of cartilage degradation and suppression of PGE(2) and MMPs expression by pomegranate fruit extract in a model of posttraumatic osteoarthritis. Nutrition 2017; 33: 1-13.
28. Gao YH, Dong N, Yang C, Li SQ, Liu JG, Qi X. Elevated synovial fluid IL-33 and IL-6 levels and cartilage degeneration in stage III osteonecrosis of the femoral head. Technol Health Care 2019.
29. Fosang AJ, Neame PJ, Last K, Hardingham TE, Murphy G, Hamilton JA. The interglobular domain of cartilage aggrecan is cleaved by PUMP, gelatinases, and cathepsin B. J Biol Chem 1992; 267: 19470-19474.
30. Burrage PS, Mix KS, Brinckerhoff CE. Matrix metalloproteinases: role in arthritis. Front Biosci 2006; 11: 529-543.
31. Bernardo MM, Fridman R. TIMP-2 (tissue inhibitor of metalloproteinase-2) regulates MMP-2 (matrix metalloproteinase-2) activity in the extracellular environment after pro-MMP-2 activation by MT1 (membrane type 1)-MMP. Biochemical Journal 2003; 374: 739-745.
32. Wang H, Sama AE. Anti-inflammatory role of fetuin-A in injury and infection. Curr Mol Med 2012; 12: 625-633.
33. Xiao J, Wang XR, Hu KZ, Li MQ, Chen JW, Ma T, et al. Serum fetuin-A levels are inversely associated with clinical severity in patients with primary knee osteoarthritis. Biomarkers 2013; 18: 51-54.
34. Jeon J, Oh H, Lee G, Ryu JH, Rhee J, Kim JH, et al. Cytokine-like 1 knock-out mice (Cytl1-

/-) show normal cartilage and bone development but exhibit augmented osteoarthritic cartilage destruction. J Biol Chem 2011; 286: 27206-27213.
35. Sieker JT, Proffen BL, Waller KA, Chin KE, Karamchedu NP, Akelman MR, et al. Transcriptional profiling of articular cartilage in a porcine model of early post-traumatic osteoarthritis. J Orthop Res 2018; 36: 318-329.
36. Huffman KM, Bowers JR, Dailiana Z, Huebner JL, Urbaniak JR, Kraus VB. Synovial fluid metabolites in osteonecrosis. Rheumatology (Oxford) 2007; 46: 523-528.
37. Narayanan A, Khanchandani P, Borkar RM, Ambati CR, Roy A, Han X, et al. Avascular Necrosis of Femoral Head: A Metabolomic, Biophysical, Biochemical, Electron Microscopic and Histopathological Characterization. Sci Rep 2017; 7: 10721.
38. Plaas AH, West LA, Wong-Palms S, Nelson FR. Glycosaminoglycan sulfation in human osteoarthritis. Disease-related alterations at the non-reducing termini of chondroitin and dermatan sulfate. J Biol Chem 1998; 273: 12642-12649.
39. Luo M, Chen J, Li S, Sun H, Zhang Z, Fu Q, et al. Changes in the metabolism of chondroitin sulfate glycosaminoglycans in articular cartilage from patients with Kashin-Beck disease. Osteoarthritis Cartilage 2014; 22: 986-995.
40. Han J, Li D, Qu C, Wang D, Wang L, Guo X, et al. Altered expression of chondroitin sulfate structure modifying sulfotransferases in the articular cartilage from adult osteoarthritis and Kashin-Beck disease. Osteoarthritis Cartilage 2017; 25: 1372-1375.
41. Zhang H, Zhang L, Wang J, Ma Y, Zhang J, Mo F, et al. Proteomic analysis of bone tissues of patients with osteonecrosis of the femoral head. OMICS 2009; 13: 453-466.
42. Luo H, Lan W, Li Y, Lian X, Zhang N, Lin X, et al. Microarray analysis of long-noncoding RNAs and mRNA expression profiles in human steroid-induced avascular necrosis of the femoral head. J Cell Biochem 2019; 120: 15800-15813.
43. Wu RW, Wang FS, Ko JY, Wang CJ, Wu SL. Comparative serum proteome expression of osteonecrosis of the femoral head in adults. Bone 2008; 43: 561-566.
44. Lafont JE, Talma S, Hopfgarten C, Murphy CL. Hypoxia promotes the differentiated human articular chondrocyte phenotype through SOX9-dependent and -independent pathways. J Biol Chem 2008; 283: 4778-4786.
45. Zhou S, Wang Z, Tang J, Li W, Huang J, Xu W, et al. Exogenous fibroblast growth factor 9 attenuates cartilage degradation and aggravates osteophyte formation in post-traumatic osteoarthritis. Osteoarthritis Cartilage 2016; 24: 2181-2192.
46. Wang Y, Sun X, Lv J, Zeng L, Wei X, Wei L. Stromal Cell-Derived Factor-1 Accelerates Cartilage Defect Repairing by Recruiting Bone Marrow Mesenchymal Stem Cells and Promoting Chondrogenic Differentiation. Tissue Eng Part A 2017; 23: 1160-1168.
47. Rowe MA, Harper LR, McNulty MA, Lau AG, Carlson CS, Leng L, et al. Reduced Osteoarthritis Severity in Aged Mice With Deletion of Macrophage Migration Inhibitory Factor. Arthritis Rheumatol 2017; 69: 352-361.

Figure 1: Schematic workflow followed in this study. Black boxes show the regions collected cartilage from the femoral head. Cartilage samples from 16 ONFH patients and matched controls were included in the study. Histological characterization of the cartilage was performed according to the HHGS score system. Then, extracted proteins were processed for TMT labeling and subsequent 2D-LC-MS/MS analysis. Bioinformatics analysis characterized the function of identified proteins and differentially expressed proteins were validated by western blot (WB) and immunohistochemical (IHC) analysis.

Figure 2: Gene ontology (GO) analysis of the DEPs in the cartilage between ONFH and the fracture control. **(A)** Top 10 significant GO terms distribution in biological process. **(B)** Top 10 significant GO terms distribution in cellular component. **(C)** Top 10 significant GO terms distribution in molecular function.

Figure 3: KEGG pathway and PPI analysis. **(A)** KEGG analysis of the DEPs in ONFH compared with fracture controls. The vertical axis shows the pathway category and name, with the *P*-value and associated protein number shown on the left, their corresponding KEGG category on the right, and the horizontal axis shows the percentage value of the proteins. **(B)** PPI networks of the DEPs in the cartilage between ONFH and the fracture control. Circle indicates proteins, rectangle indicates KEGG pathway or biological process. Pathway were colored with gradient color from yellow to blue which indicates *P*-value from low to high. In case of fold change analysis, red indicates up-regulated proteins and green indicates down-regulation. Default confidence cutoff of 400 was used: interactions with bigger confident score were show as solid lines, otherwise in dashed lines.

Figure 4: Western blot of two DEPs. Relative intensities of the positively identified proteins are shown by the dot plots. Patients with ONFH displayed higher levels of AHSG **(A)** and lower levels of Cytl1 **(B)**. The relative density was calculated by dividing the density of matched spot by the density of the matched spots in the reference gel. **P*-value < 0.05, ** *P*-value < 0.01.

Figure 5: Immunohistochemistry results for Alpha-2-HS-glycoprotein (AHSG) **(A)** and Cytokine-like protein 1 (Cytl1) **(B)** proteins in hip cartilage from ONFH patients and fracture control. Original magnification ×200 of the superficial zone (SZ) and deep zone (DZ). **P*-value < 0.05, ** *P*-value < 0.01.

Figure S1: Principal components analysis (PCA) analysis between ONFH and fracture control group. PCA showed the homogeneity and heterogeneity in and between ONFH and fracture control group.

Figure S2: Immunohistochemistry results for aggrecan and MMP13 of articular cartilage in fracture control and ONFH group. Original magnification ×200 of the superficial zone (SZ) and deep zone (DZ). ^{NS} *P*-value > 0.05, **P*-value < 0.05, *** *P*-value < 0.001.

Figure S3: Safranin O (SO) and toluidine blue (TB) staining of articular cartilage in fracture control and ONFH group. In ONFH groups, the rates of intensive staining area were much lower in all 2 layers compared with the control group. Original magnification ×200 of the superficial zone (SZ) and deep zone (DZ). ***P*-value < 0.01, *** *P*-value < 0.001.

Table 1 Basic characteristics of the study subjects

Patient ID	ONFH				Fracture control			
	Age (years)	Gender	BMI (kg/m^2)	TMT label	Age (years)	Gender	BMI (kg/m^2)	TMT label
TMT analysis								
1	56	Male	24.2		61	Male	23.4	
2	51	Male	23.5	128C	61	Male	24.6	127N
3	52	Female	23.8		65	Female	22.6	
4	46	Male	21.5		60	Male	24.2	
5	55	Male	24.3	129N	59	Male	25.1	127C
6	50	Female	20.3		63	Female	20.8	
7	50	Male	22.9		60	Male	23.6	
8	45	Male	25.3	130N	57	Male	21.2	126
9	48	Female	22.7		62	Female	22.0	
WB								
10	53	Male	26.1	-	64	Male	26.4	-
11	45	Male	23.4	-	61	Male	23.8	-
12	47	Female	23.3	-	65	Female	21.6	-
13	38	Female	24.8	-	63	Female	24.0	-
IHC								
14	50	Male	20.9	-	65	Male	22.0	-
15	47	Male	23.0	-	61	Male	22.9	-
16	52	Female	19.2	-	61	Female	19.5	-

ONFH, osteonecrosis of the femoral head; WB, western blot; IHC, immunohistochemistry; BMI, body mass index.

$P_{BMI,TMT} = 0.879$, $P_{BMI,WB} = 0.717$, $P_{BMI,IHC} = 0.787$; $P_{age,TMT} < 0.001$, $P_{age,WB} < 0.01$, $P_{age,IHC} < 0.05$.

Table 2 Top 20 up regulated differentially expressed proteins in ONFH cartilage

Accession	Protein name	Gene name	Peptides	Coverage [%]	Mascot Score	FC P/C	*P* value
A0A0A0MS15	Immunoglobulin heavy variable 3-49	IGHV3-49	2	17	76	5.14227	0.0112
P02765	Alpha-2-HS-glycoprotein	AHSG	9	28	394	4.64972	0.02509
Q15582	Transforming growth factor-beta-induced protein ig-h3	TGFBI	20	34	746	4.45951	0.04382
P45452	Collagenase 3	MMP13	4	11	123	3.47761	0.00621
P02790	Hemopexin	HPX	12	34	536	3.33526	0.01126
P20851	C4b-binding protein beta chain	C4BPB	1	5	0	3.30488	0.03746
Q15166	Serum paraoxonase/lactonase 3	PON3	1	2	33	3.30179	0.03592
Q9BW30	Tubulin polymerization-promoting protein family member 3	TPPP3	5	29	124	3.1965	0.04802
Q16610	Extracellular matrix protein 1	ECM1	10	22	276	3.158	0.02544
P02787	Serotransferrin	TF	39	60	2106	3.12371	0.03781
P20908	Collagen alpha-1(V) chain	COL5A1	12	7	324	3.11309	0.0017
P41222	Prostaglandin-H2 D-isomerase	PTGDS	1	9	101	3.05064	0.01299
Q8IUX7	Adipocyte enhancer-binding protein 1	AEBP1	26	26	719	3	0.03117
P08253	72 kDa type IV collagenase	MMP2	23	39	677	2.89799	0.01138
P19652	Alpha-1-acid glycoprotein 2	ORM2	6	31	241	2.87783	0.04716
P02647	Apolipoprotein A-I	APOA1	17	64	798	2.80469	0.00804
P02652	Apolipoprotein A-II	APOA2	3	37	82	2.72965	0.03441
P04003	C4b-binding protein alpha chain	C4BPA	14	28	361	2.64299	0.04813
Q9H4F8	SPARC-related modular calcium-binding protein 1	SMOC1	12	27	231	2.56871	0.00139

FC, fold change. P/C, protein abundance in patient/protein abundance in control.

Table 3 Top 20 down regulated differentially expressed proteins in ONFH cartilage

Accession	Protein name	Gene name	Peptides	Coverage [%]	Mascot Score	FC P/C	*P* value
P02776	Platelet factor 4	PF4	4	43	125	0.09771	0.001
P0DJI8	Serum amyloid A-1 protein	SAA1	4	42	98	0.19241	0.04284
P02788	Lactotransferrin	LTF	20	36	685	0.23305	0.00674
P20160	Azurocidin	AZU1	1	4	45	0.23941	0.00573
Q13061	Triadin	TRDN	2	2	31	0.26236	0.03582
Q6UXI7	Vitrin	VIT	16	27	598	0.27044	0.03074
P46976	Glycogenin-1	GYG1	5	17	218	0.29422	0.00082
P80188	Neutrophil gelatinase-associated lipocalin	LCN2	4	24	146	0.30067	0.04191
P06702	Protein S100-A9	S100A9	4	38	157	0.30067	0.00226
P83105	Serine protease HTRA4	HTRA4	1	1	39	0.30969	0.00622
P02775	Platelet basic protein	PPBP	7	50	163	0.31055	0.00876
Q9NRY4	Rho GTPase-activating protein 35	ARHGAP35	1	0	46	0.31817	0.00596
P05109	Protein S100-A8	S100A8	7	56	81	0.32093	0.00127
P36222	Chitinase-3-like protein 1	CHI3L1	11	37	431	0.32685	0.00023
P26583	High mobility group protein B2	HMGB2	2	11	85	0.3366	0.01119
Q9GZM7	Tubulointerstitial nephritis antigen-like	TINAGL1	1	3	60	0.34086	0.01317
Q9BQB4	Sclerostin	SOST	6	28	70	0.34439	0.01156
P05783	Keratin, type I cytoskeletal 18	KRT18	3	7	87	0.35708	0.00088
Q7Z7L8	Uncharacterized protein C11orf96	C11orf96	2	4	45	0.36054	0.04401

FC, fold change. P/C, protein abundance in patient/protein abundance in control.

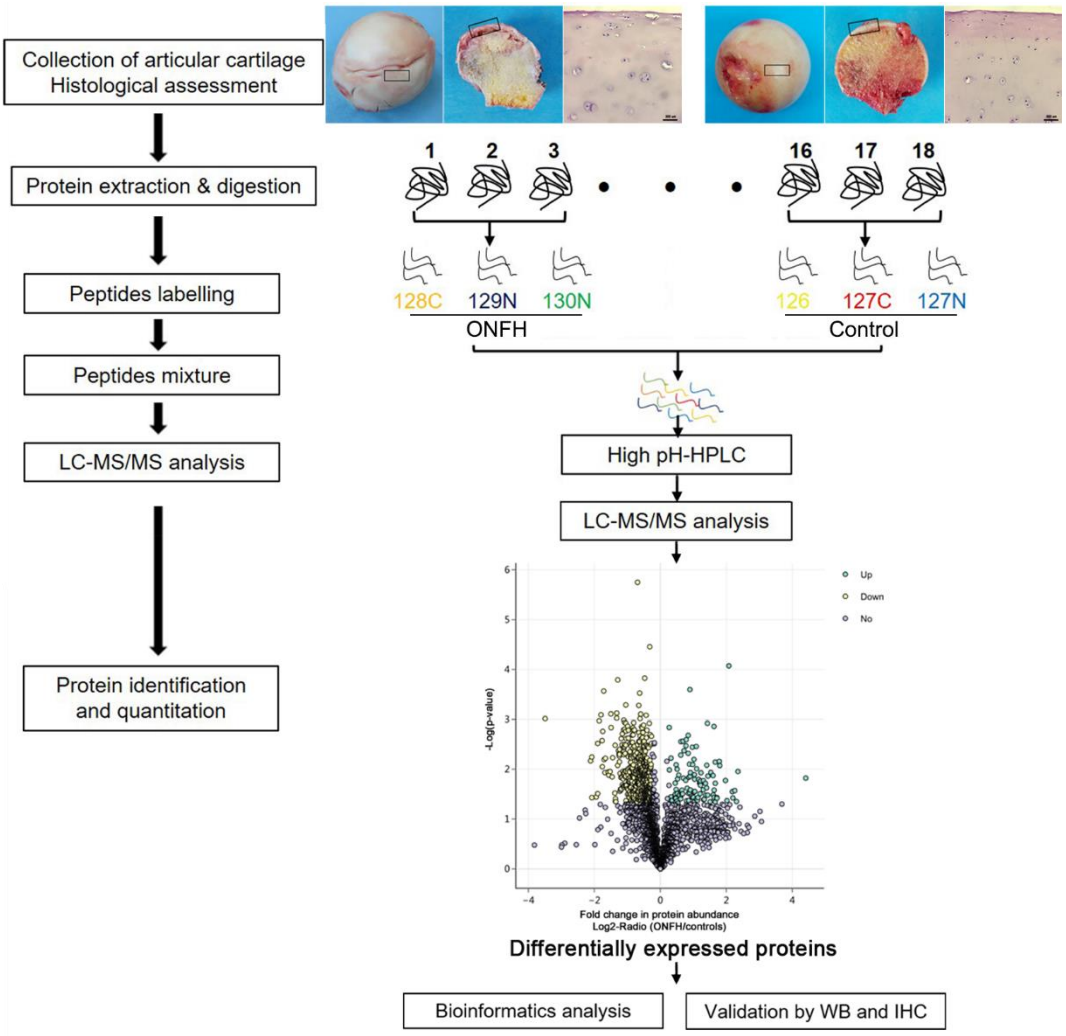
Collection of articular cartilage
Histological assessment
Protein extraction & digestion
Peptides labelling
Peptides mixture
LC-MS/MS analysis
Protein identification
and quantitation
1
2
3
16
17
18
128C
129N
130N
126
127C
127N
ONFH
Control
High pH-HPLC
LC-MS/MS analysis
Up
Down
No
-Log(p-value)
Fold change in protein abundance
Log2-Radio (ONFH/controls)
Differentially expressed proteins
Bioinformatics analysis
Validation by WB and IHC

Figure 1

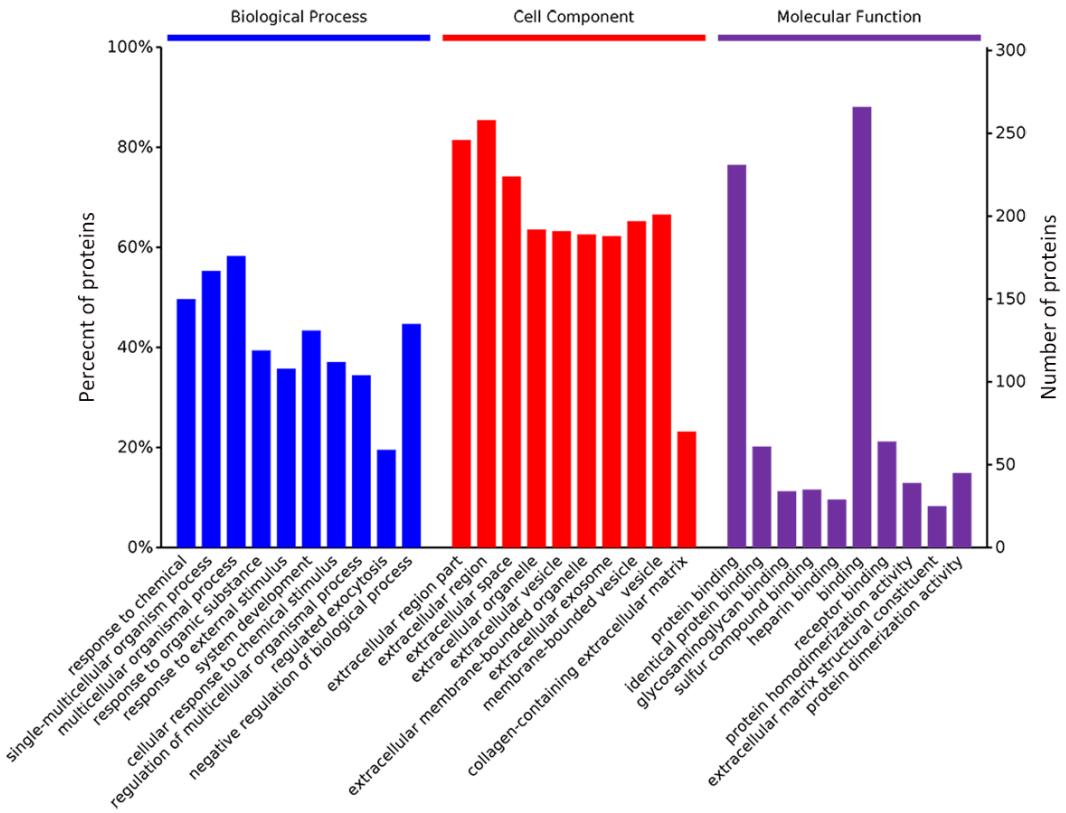
Biological Process
Cell Component
Molecular Function
Percecnt of proteins
Number of proteins
100%
80%
60%
40%
20%
0%
300
250
200
150
100
50
0
response to chemical
single-multicellular organism process
multicellular organismal process
response to organic substance
response to external stimulus
system development
cellular response to chemical stimulus
regulation of multicellular organismal process
negative regulation of biological process
regulated exocytosis
extracellular region part
extracellular region
extracellular space
extracellular organelle
extracellular vesicle
extracellular membrane-bounded organelle
extracellular exosome
membrane-bounded vesicle
collagen-containing extracellular matrix
vesicle
protein binding
identical protein binding
glycosaminoglycan binding
sulfur compound binding
heparin binding
binding
receptor binding
protein homodimerization activity
extracellular matrix structural constituent
protein dimerization activity

Figure 2

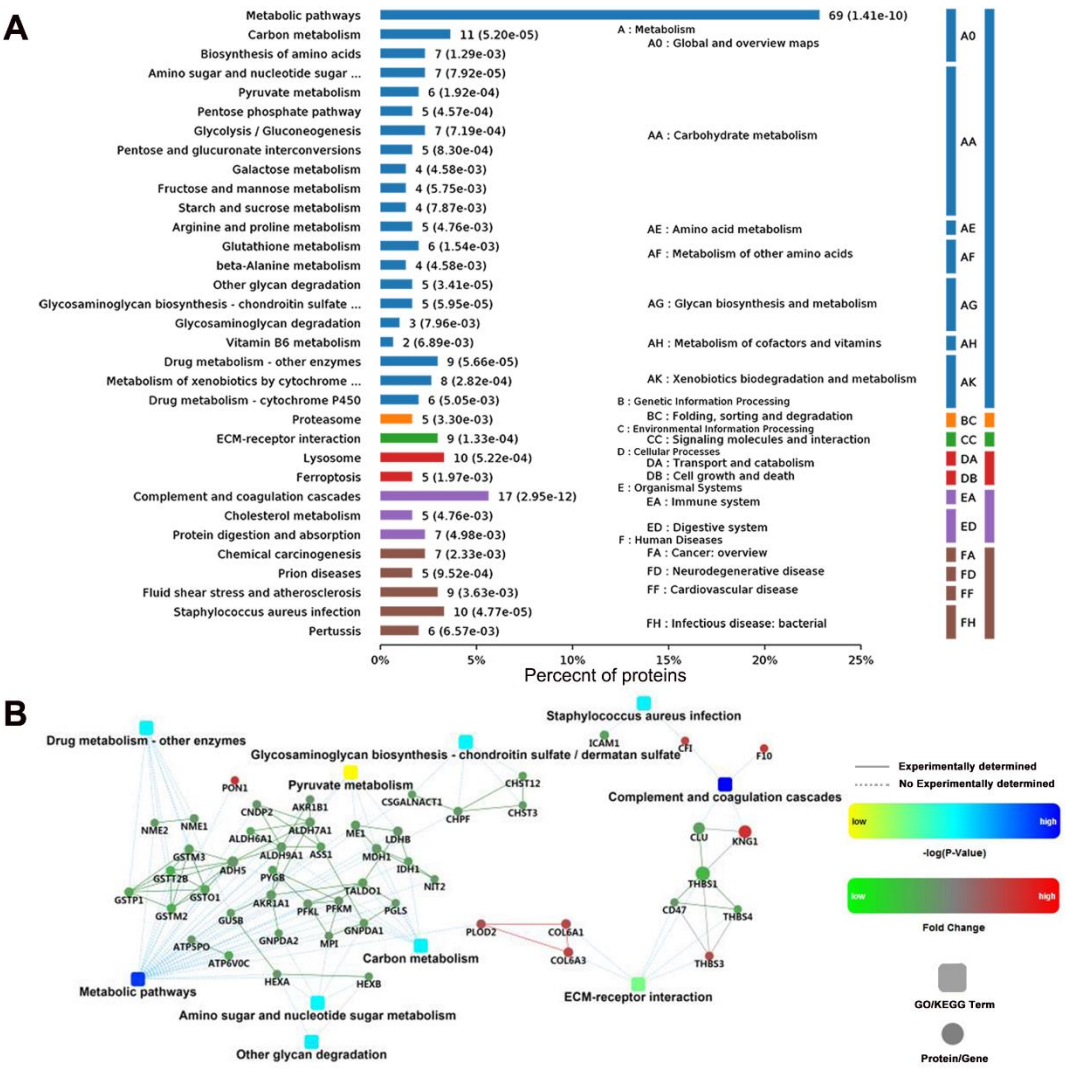
A
Metabolic pathways
Carbon metabolism
Biosynthesis of amino acids
Amino sugar and nucleotide sugar ...
Pyruvate metabolism
Pentose phosphate pathway
Glycolysis / Gluconeogenesis
Pentose and glucuronate interconversions
Galactose metabolism
Fructose and mannose metabolism
Starch and sucrose metabolism
Arginine and proline metabolism
Glutathione metabolism
beta-Alanine metabolism
Other glycan degradation
Glycosaminoglycan biosynthesis - chondroitin sulfate ...
Glycosaminoglycan degradation
Vitamin B6 metabolism
Drug metabolism - other enzymes
Metabolism of xenobiotics by cytochrome ...
Drug metabolism - cytochrome P450
Proteasome
ECM-receptor interaction
Lysosome
Ferroptosis
Complement and coagulation cascades
Cholesterol metabolism
Protein digestion and absorption
Chemical carcinogenesis
Prion diseases
Fluid shear stress and atherosclerosis
Staphylococcus aureus infection
Pertussis
69 (1.41e-10)
11 (5.20e-05)
7 (1.29e-03)
7 (7.92e-05)
6 (1.92e-04)
5 (4.57e-04)
7 (7.19e-04)
5 (8.30e-04)
4 (4.58e-03)
4 (5.75e-03)
4 (7.87e-03)
5 (4.76e-03)
6 (1.54e-03)
4 (4.58e-03)
5 (3.41e-05)
5 (5.95e-05)
3 (7.96e-03)
2 (6.89e-03)
9 (5.66e-05)
8 (2.82e-04)
6 (5.05e-03)
5 (3.30e-03)
9 (1.33e-04)
10 (5.22e-04)
5 (1.97e-03)
17 (2.95e-12)
5 (4.76e-03)
7 (4.98e-03)
7 (2.33e-03)
5 (9.52e-04)
9 (3.63e-03)
10 (4.77e-05)
6 (6.57e-03)
A : Metabolism
A0 : Global and overview maps
AA : Carbohydrate metabolism
AE : Amino acid metabolism
AF : Metabolism of other amino acids
AG : Glycan biosynthesis and metabolism
AH : Metabolism of cofactors and vitamins
AK : Xenobiotics biodegradation and metabolism
B : Genetic Information Processing
BC : Folding, sorting and degradation
C : Environmental Information Processing
CC : Signaling molecules and interaction
D : Cellular Processes
DA : Transport and catabolism
DB : Cell growth and death
E : Organismal Systems
EA : Immune system
ED : Digestive system
F : Human Diseases
FA : Cancer: overview
FD : Neurodegenerative disease
FF : Cardiovascular disease
FH : Infectious disease: bacterial
A0
AA
AE
AF
AG
AH
AK
BC
CC
DA
DB
EA
ED
FA
FD
FF
FH
0%
5%
10%
15%
20%
25%
Percecnt of proteins
B
Staphylococcus aureus infection
Drug metabolism - other enzymes
Glycosaminoglycan biosynthesis - chondroitin sulfate / dermatan sulfate
Pyruvate metabolism
Complement and coagulation cascades
Carbon metabolism
Metabolic pathways
Amino sugar and nucleotide sugar metabolism
Other glycan degradation
ECM-receptor interaction
Experimentally determined
No Experimentally determined
low
high
-log(P-Value)
Fold Change
GO/KEGG Term
Protein/Gene

Figure 3

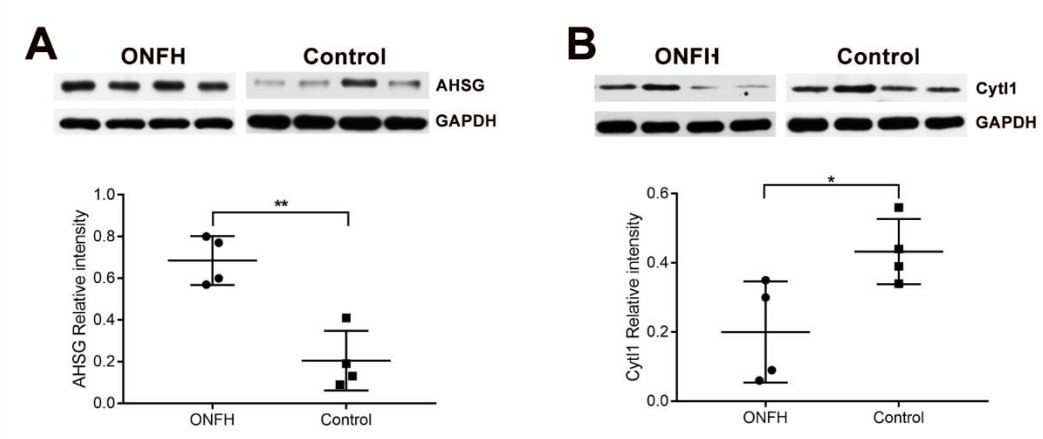

682
683
684 **Figure 4**
685
686

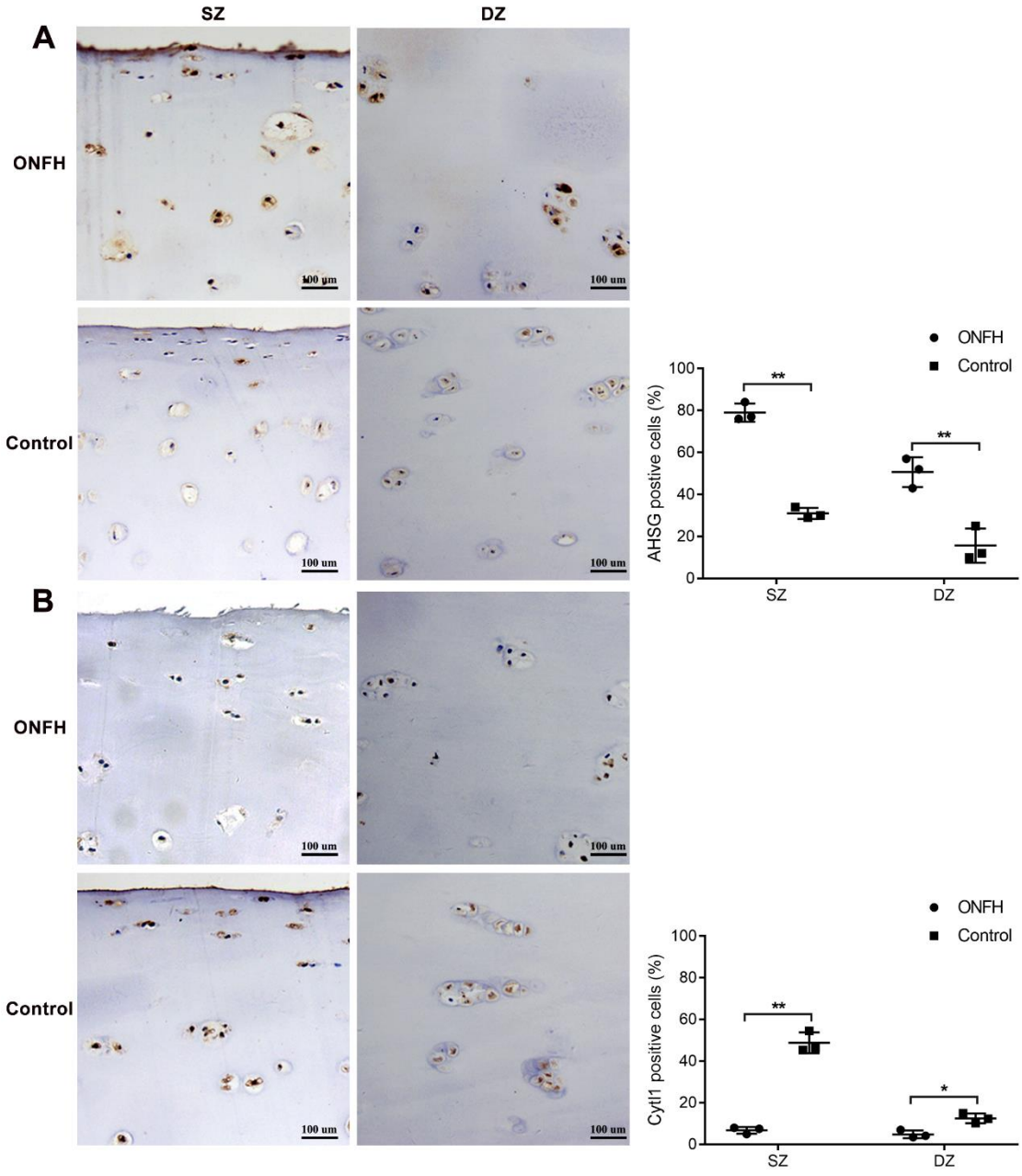
SZ
DZ
A
ONFH
Control
100 um
B
ONFH
Control
AHSG postive cells (%)
ONFH
Control
**
**
100
80
60
40
20
0
SZ
DZ
Cytl1 positive cells (%)
ONFH
Control
**
*
100
80
60
40
20
0
SZ
DZ

Figure 5

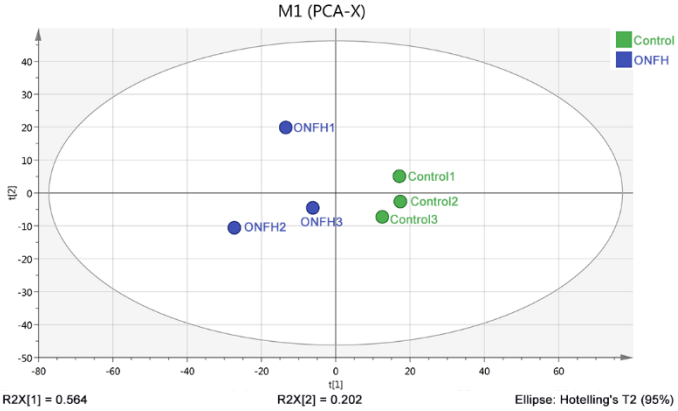

692

693 **Figure S1**

694

695 **f**

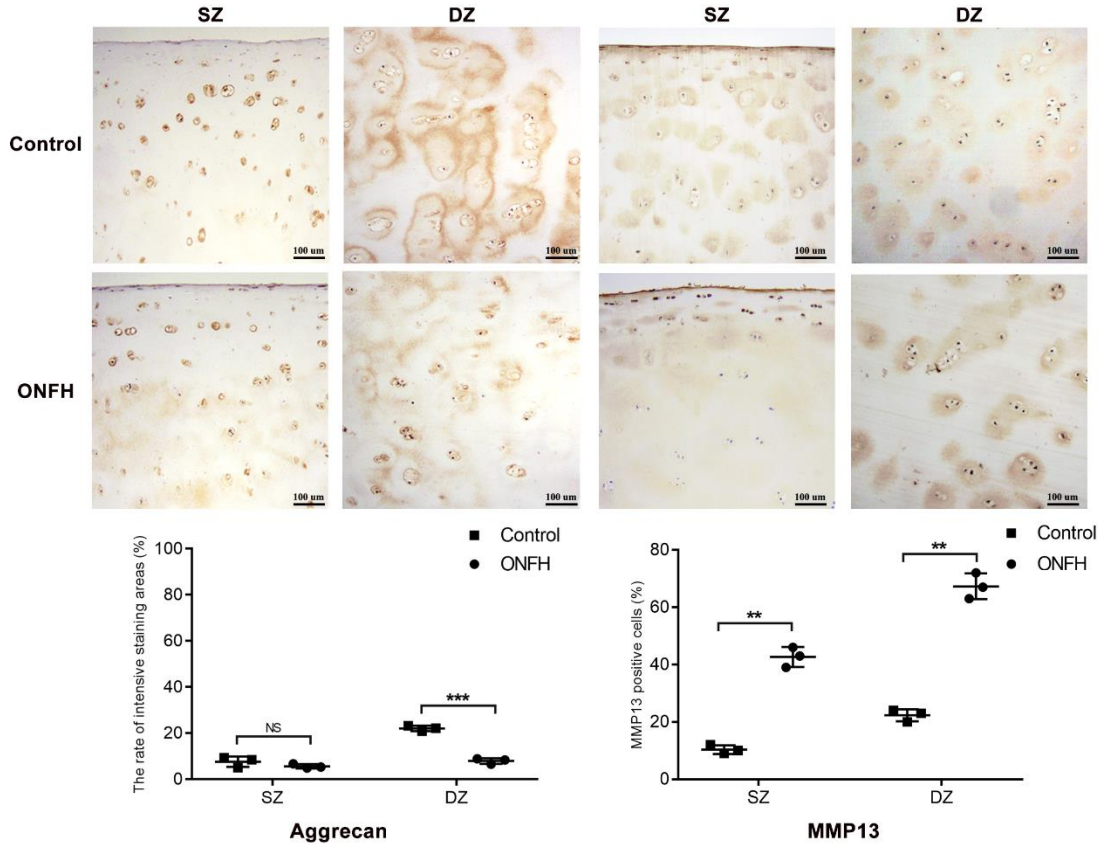

696

697 **Figure S2**

698

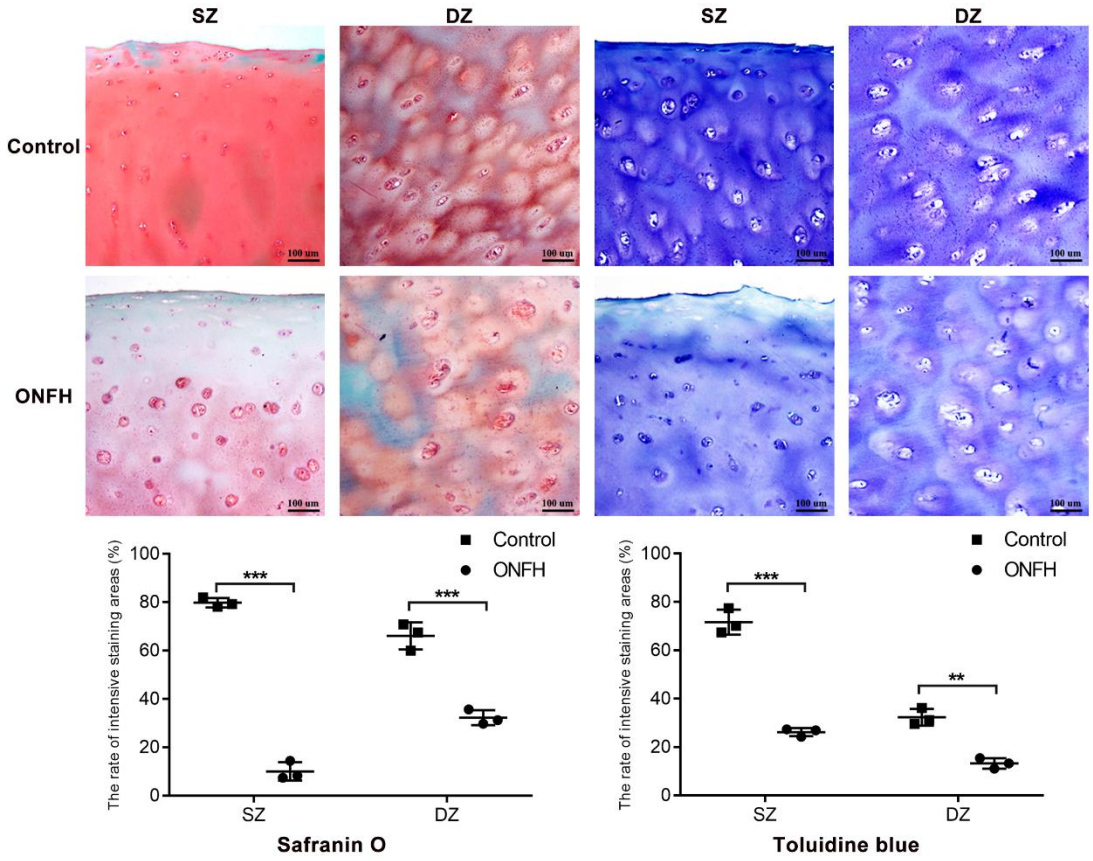
SZ
DZ
SZ
DZ
Control
ONFH
100 um
Control
ONFH
The rate of intensive staining areas (%)
100
80
60
40
20
0
***
***
SZ
DZ
Safranin O
Control
ONFH
The rate of intensive staining areas (%)
100
80
60
40
20
0
***
**
SZ
DZ
Toluidine blue

Figure S3